



# Identification of Extremely Virulent Infectious Bursal Disease Virus Via Molecular and Histological Methods in Broiler Chickens

Ammar Taleb Nasser<sup>1</sup> , Amer Al-Azzawi<sup>1</sup> ; Ramzi Al-Agele<sup>1</sup> , and Karim Al-Ajeeli<sup>2</sup> 

<sup>1</sup>Department of Microbiology, College of Veterinary Medicine, Diyala University, Diyala, Iraq

<sup>2</sup>Department of Anatomy and Histology, College of Veterinary Medicine, Diyala University, Diyala, Iraq

\*Corresponding author's E-mail: Amer\_alazawy@yahoo.com

Received: January 03, 2024, Revised: February 25, 2024, Accepted: March 10, 2024, Published: March 25, 2024

## ABSTRACT

Infectious bursal disease (IBD) is caused by an RNA virus belonging to the Avibirnavirus genus within the Birnaviridae family. The global prevalence of infectious bursal disease virus (IBDV) is a significant concern, affecting birds of all ages. Birds infected with IBDV exhibit symptoms, such as depression, bleeding in the thighs and pectoral muscles, and enlargement of the bursa. This study aimed to identify predominant IBDV serotypes using molecular methods and to gain insights into the resulting pathological conditions in infected chickens. Additionally, the study investigated the viral sequence and the relationship between a local Diyala isolate and reference strains from the Genbank. In the current study, the IBDV was isolated from broiler chickens aged 2-3 weeks from 15 farms in the Diyala Governorate of Iraq. A total of 15 samples, each from a different farm, were collected. Necropsy samples were obtained from various organs of broiler chickens, including the bursa of Fabricius, lungs, liver, and kidneys. Specific primers targeting the VP2 gene were used for reverse transcription-polymerase chain reaction (RT-PCR) analysis. The RT-PCR analysis yielded a 727 bp fragment, confirming the presence of IBDV in 10 out of the 15 samples. One strain was assigned the accession number LC498531 in the NCBI database. Phylogenetic analysis using the neighbor-joining tree program revealed three distinct groups. All examined regional samples (S1) were situated within the constructed tree. Five samples formed a specific group, indicating a close relationship. Histological examination of the tissues showed visible alterations such as degeneration, necrosis, and infiltration of inflammatory cells, particularly heterophils, providing clear evidence of the disease. In conclusion, this study confirmed the presence of IBDV in broiler chickens from multiple farms in Iraq's Diyala Governorate, highlighting distinct clustering patterns in viral sequences. Moreover, the study confirmed the virus's presence using conventional RT-PCR, with histological examination supporting the findings.

**Keywords:** Broiler chicken, Bursal enlargement, Infectious bursal disease, RT-PCR

## INTRODUCTION

The infectious bursal disease virus (IBDV), belonging to the genus Avibirnavirus within the Birnaviridae family, has an RNA genome. This virus is responsible for causing infectious bursal disease (IBD; Fauquet and Mayo, 2001). The IBDV has a single, icosahedral-symmetric capsid envelope with 32 capsomeres that are between 55 and 60 nm in diameter. The virus is non-enveloped and double-stranded (Fauquet and Mayo, 2001). The IBD is a highly transmissible disease that mainly strikes chickens leading to immunosuppression and increased susceptibility to secondary infections. This immunosuppression hampers

effective immunization against other diseases, such as infectious bronchitis, Marek's disease, and Newcastle disease, therefore making chickens more susceptible to these opportunistic diseases (Allan et al., 1972; Lasher and Shane, 1994). While IBD is commonly observed in chickens worldwide, other bird species, such as ostriches, guinea fowl, turkeys, and ducks can be infected without showing apparent clinical symptoms. The presence of IBD poses a significant threat to the global poultry industry, leading to reduced profitability and hindering its expansion (Dye et al., 2019; Zhang et al., 2022). The disease was first identified in a broiler flock in Sussex, USA, and later named "Gumboro" following an outbreak

reported in the Gumboro region of southern Delaware, USA. Infected birds exhibit a distinctive lesion termed “avian nephrosis” that primarily affects the kidneys (Rauf et al., 2011; Dey et al., 2019). Remarkably, antigenic variant strains can evade cross-neutralization antisera against classical strains. In contrast, extremely virulent strains can infect birds even in the presence of high levels of previously protective maternally derived antibodies (MDA) against classical strains. (Jackwood and Sommer-Wagner, 2007). In the case of IBD, two distinct periods of occurrence exist, dependent on the age of the chickens (Dey et al., 2019). During the first period, the disease is noticed in birds younger than 3 weeks old, and infected chickens show few clinical signs but are grossly characterized by bursa atrophy, which causes severe immunosuppression. The clinical form of IBD affects poultry aged between 3 and 6 weeks. Affected chickens show signs, such as ruffled feathers, watery droppings, urate accumulation in their kidneys and urinary tubules, loss of appetite, depression, trembling, extreme prostration, and ultimately death (Lukert and Saif, 2003; Ingrao et al., 2013). The IBDV is categorized into two serotypes, namely serotype I and serotype II. Serotype I is pathogenic to broiler and layer chickens, while serotype II is considered non-pathogenic or of low virulence (Al-Sheikhly et al., 1978; Wang et al., 2009). Serotype I is the predominant worldwide serotype associated with severe clinical disease, and consequently, all vaccines are developed based on this serotype (Dey et al., 2019). Serotype I viruses can be divided into four subtypes based on changes in antigenicity and virulence, namely classic strains, antigenically variable strains, extremely virulent strains, and attenuated IBDV (Cao et al., 1998). The IBDV genome consists of five proteins known as VP1-VP5, with two segments, A and B. Segment A contains the genetic information for two structural proteins, VP2 and VP3, along with two non-structural proteins, VP4 and VP5 (Ferrero et al., 2015). According to Raja et al. (2016) and Deorao et al. (2021), segment B encodes the non-structural protein VP1, which is a representation of viral transcripts. A host-protective virus with at least three neutralizing epitopes is thought to have VP2 as its primary antigen (Coulibaly et al., 2005). A limited scope of minor amino acid variation is observed in the variable region of the VP2 gene, and this variation may be the cause of the development of antigenic variants in all IBDV strains.

The highly variable region (HVR) plays a critical role in stimulating the production of antibodies that neutralize viruses due to the presence of different epitopes stimulating their production (Lukert and Saif, 2003). One

of the major challenges facing chicken farmers in Iraq, particularly in the Diyala Governorate located in eastern Iraq, is infectious bursal disease caused by the virus. However, little is known about the histological alterations accompanying the disease or the molecular evidence of IBDV in this region. The aim of this study was to examine the molecular evidence and histological changes linked to IBDV in broiler flocks from selected farms in the Diyala Governorate of Iraq.

## **MATERIALS and METHODS**

### **Ethical approval**

The research received approval from the Scientific Ethics Council, and the study's ethical number, Vet Medicine 301 August 2019 A, A, R, and K, was validated at the University of Diyala/College of Veterinary Medicine in Iraq.

### **Study area**

This study was conducted in the molecular biology and virology labs of the College of Veterinary Medicine at the University of Diyala in Iraq.

### **Molecular detection**

Reverse transcriptase polymerase chain reaction (RT-PCR) was employed to track the molecular detection of IBDV. Fifteen tissue samples were collected, each comprising the liver, spleen, kidney, and bursa of Fabricius from broiler chickens diagnosed with severe IBDV infections during necropsies at the age of 2-3 weeks. Tissue samples (one from each bird) were extracted for viral RNA from the kidneys, spleen, liver, and bursa of Fabricius using an extraction kit for tissue (Kylt® RNA / DNA Purification kit, Germany) according to the manufacturer's instructions. Sterile plastic containers were utilized to store the samples, which were then placed in Falcon tubes and kept at -20°C in a deep freezer until required. Infected chickens with IBDV indicated a severe infection and high mortality rate. During necropsy, the bursa of Fabricius showed inflammation with varying degrees of hemorrhage, edema, and follicles filled with gelatinous exudates. Ecchymotic hemorrhages were also observed on the thigh and breast muscles (See Figures 1 and 2).

As previously described by Meir et al. (2001), a set of publishing oligonucleotide primers selected from a highly conserved region was purchased from Microgen, Korea, and used for the detection of IBDV. A commercially available kit (Promega, USA) and PCR reaction mixtures prepared in a 25 Eppendorf tube were used to amplify a

727-bp fragment targeting specific genes within the VP2 region. These primers included IBDV-F (5-CAGGTGGGGTAACAACAATCA-3) and IBDV-R (5-CGGCAGGTGGGAACAATG-3) using Access RT-PCR System and RNasin® Ribonuclease Inhibitor kit (Promega®, Madison, USA). After a quick spin for a few seconds, the RT-PCR tubes were placed in an Eppendorf thermal cycler (USA) and run through 40 cycles of the following temperature profile for product detection. The RT-PCR was run for 10 minutes at an RT reaction temperature of 50°C. After that, 40 cycles of denaturation at 95°C for 1 minute, annealing at 59°C for 40 seconds, and extension at 720°C for 1 minute were carried out consecutively, with the last extension lasting 10 minutes at 72°C. After RT-PCR, the products from the 15 samples were subjected to electrophoresis. Following the staining of the DNA with a red dye, the amplified fragments became visible on gel electrophoresis (Meir et al., 2001).

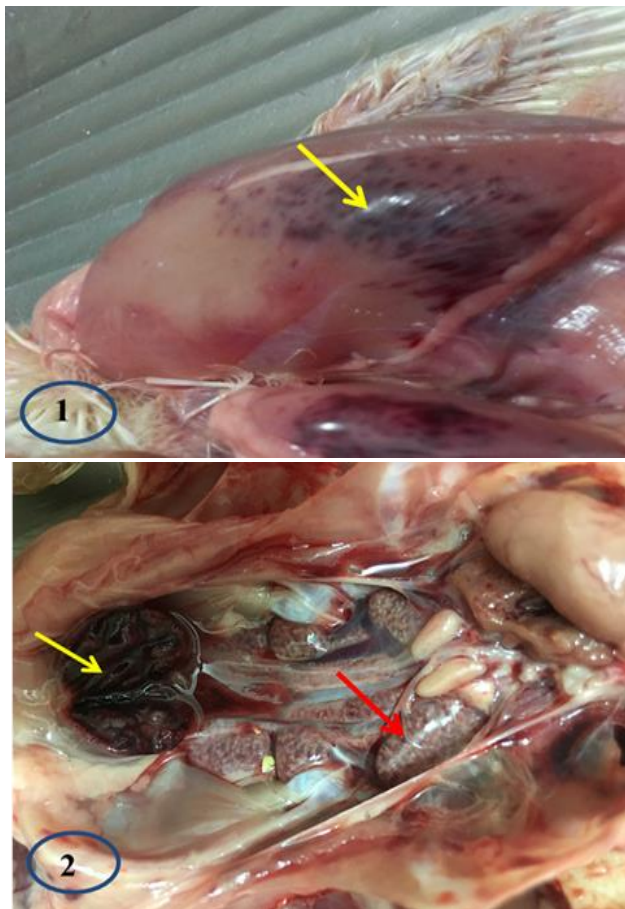


**Figure 1.** A boiler chicken suspected to infectious bursal disease virus. **1:** Ecchymotic hemorrhages on the thigh and breast muscles (yellow arrow). **2:** Congestion and bleeding on the bursal's serosal surface (yellow arrow), and kidneys swollen with urates (red arrow).

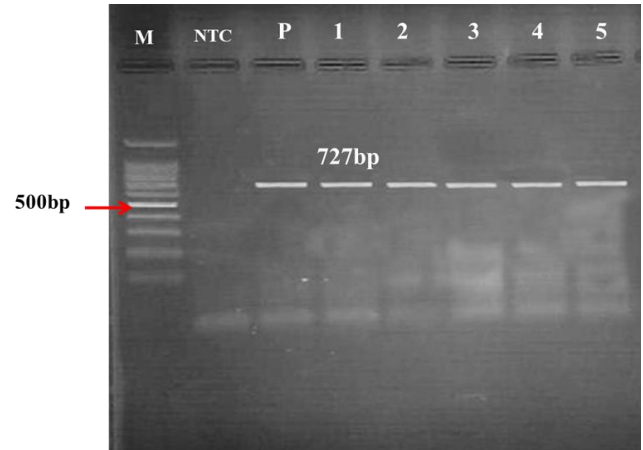


**Figure2.** Tissue samples of broiler chickens suspected to infectious bursal disease virus using RT-PCR and oligonucleotide primers (IBDV-F and IBDV-R) produced the target band of approximately 727bp stained by Red stain. **M:** DNA ladder (1000 bp); **NTC:** Non-template control; **P:** Positive control; **Lanes 1-5:** Positive samples from chickens infected with IBDV.

#### DNA sequencing of PCR amplicon

Following the guidelines provided by the sequencing company (Macrogen Inc., Geumchen, Seoul, South Korea), the 727 bp resolved PCR amplicons were commercially sequenced from both termini (forward and reverse). To ensure that annotation and variations were not the result of PCR or sequencing artifacts, only clear chromatographs obtained from ABI (Applied Biosystems) sequence files were analyzed. Virtual positions and other information of the retrieved PCR fragments were identified by comparing the observed DNA sequences of the viral samples with the retrieved DNA sequences of the viral database. Through a comparison of DNA chromatograms with the viral DNA sequences that were deposited using BioEdit versus 7.1 (DNASTAR, Madison), nucleic acid variations were made evident. Every variety found within the IBDV genes was annotated by SnapGene Viewer ver. 4.0.4 (Jasim et al., 2022).

#### Phylogenetic trees

In this study, a specific and comprehensive tree was constructed using the neighbor-joining method. Detected variations were then compared to nearby homologous reference sequences using the NCBI-BLASTn server (Zhang et al., 2000). Next, using the neighbor-joining technique, circular trees were constructed, including the variant that was observed. Using the iTOL suit, each generated form was annotated as a cladogram (Letunic and Bork, 2019). To determine the precise genotype of the

IBDV samples in the present study, multiple reference sequences representing each of the three IBDV genotypes were provided. Each phylogenetic genetic group's sequences in the tree were colored according to their classification.

### **Histopathology**

Thirty Infected chickens with IBD were humanely euthanized with a high dose of ketamine (50mg/kg) and xylazine (5mg/kg; Kadhim et al., 2023). After that, an incision and dissection were made in abdominal regions, followed by tissue samples (6 mm thick) from different regions of the bursa of Fabricius, lungs, liver, and kidneys, which were removed and immediately immersed in the 10% fixative formalin solution for 24 hours at room temperature. Then, all tissue samples were processed by routine methods, embedded in paraffin wax, sectioned at 5 mm, and stained with routine staining (H&E). In the next step, photomicrographs were captured of each histological field (Aliyu et al., 2022).

## **RESULTS**

### **Molecular detection**

Fifteen extracted RNA samples from respective cases designated as Diyala isolates were screened by RT-PCR assay to detect IBDV. The oligonucleotide primer sequences were chosen from a highly conserved region essentially the hypervariable VP2 region. On a 2% agarose gel, all the amplified cDNA displayed the same mobility. Ten out of 15 samples (66.66%) were positive for IBDV. As seen in Figure 2, positive samples produced a distinct DNA band with a length of 727 bp.

One strain was registered in NCBI and received an accession number (LC498531). Following comparison with all reference strains available from GenBank.

### **Sequencing results**

Following an NCBI blast analysis, the sequencing reactions accurately pinpointed the locations of the examined samples. Upon comparing the sequenced samples with the expected target, which encompassed the VP2 locus within the IBDV sequences, this method demonstrated the highest similarity. The precise locations and additional details of the retrieved PCR fragment were determined by comparing the observed DNA sequences of these viral samples with the reference sequences retrieved. With the GenBank accession number LC498531.1, the NCBI BLASTn engine revealed up to 98% homology with these predicted targets that covered designated regions of VP2 sequences (Figure 3).

After positioning the 727 bp amplicon sequences within the VP2 locus of IBDV sequences, detailed information was provided, including the positions of the forward and reverse primers within the targeted IBDV sequences (Table 1).

Alignment results of the 727 bp sample revealed the detection of 13 nucleic acid variations in comparison with referring sequences of the IBDV sequences (Figure 4). The results indicated the presence of 13 nucleic acid variants in the S1 local sample as compared to reference sequences of the IBDV (GenBank acc. no. LC498531.1). Investigated nucleic acid sequences were converted to their corresponding positions in the IBDV coat protein VP2. All nucleic acid sequences of investigated local samples were translated to their corresponding amino acid sequences using the ExPasy translate suite. Amino acid alignment of these amino acid sequences with its reference sequences indicated that investigated 727 bp amplicons had consisted of 242 amino acid sequences in entire amino acid sequences in VP2 in IBDV (Figure 5). It was found that all detected variants had caused a silent effect on the VP2 protein.

A detailed description of identified variations in the investigated S1 local sample was presented in Table 2. Based on the nucleic acid sequences found in the examined sample, an inclusive phylogenetic tree was created in the current investigation. The S1 local sample of IBD virus sequences was included in this phylogenetic tree along with other relevant NCBI reference sequences. Due to the presence of several clades of the IBDV, a direct comparison between present samples with the previously known reference genotypes was conducted to find out the accurate positioning of the samples within the main clades of these viral particles. As a result, the viral isolate was directly compared to several representative reference samples coming from different viral variations inside the phylogenetic tree that was produced. It was possible to determine their actual evolutionary distances with greater accuracy as a result. In this extensive tree, 38 aligned nucleic acid sequences were present. This created three indicated the presence of several significant clades, and the viral sample under investigation was included in one of them. The clear phylogenetic information of this researched IBDV was disclosed, as deduced from the VP2-based tree.

The currently constructed tree was represented in two cladograms, which were made to generate a circular cladogram (Figure 6). In each generated form, a particular phylogenetic distribution of incorporated sequences was notified. The presence of the most common clades of IBDV was carried out to provide reference sequences for a more thorough analysis of the evolutionary relationships among the examined viral organisms. Using this neighbor-joining tree, three distinct phylogenetic groups were observed. Within one of the IBDV-VP2 clades, the investigated viral sample was incorporated. It was found

that all investigated samples of S1 were incorporated within a specific position of the constructed tree within a clade made of five samples. Within this clade, it should be noted that all these five samples were suited in the vicinity of variable reference sequences deposited from variable IBDV strains of India (GenBank KX223749.1), Tanzania (GenBank AB368970.1), Hungary (GenBank ON100651.1), and Egypt (GenBank KY610528.1) origins within this clade. However, no close phylogenetic positioning of the local sample toward these isolates was found. Due to the identified three nucleic acid

substitutions, the obvious deviation was observed for the S1 sample compared to these reference samples. This data indicated the significant effects of the identified variants in inducing clear phylogenetic alterations within the generated tree. To indicate the ability of such genetic sequences to explain different IBDV mutations utilizing this genetic fragment, an inclusive tree has been created. This further demonstrates the effectiveness of the VP2-specific primers currently in use in locating the phylogenetic clustering of the virus isolates causing IBD that is being studied.

### Infectious bursal disease virus strain Al-Azzawi.A.K gene for VP2, partial cds

GenBank: LC498531.1

[GenBank](#) [FASTA](#)

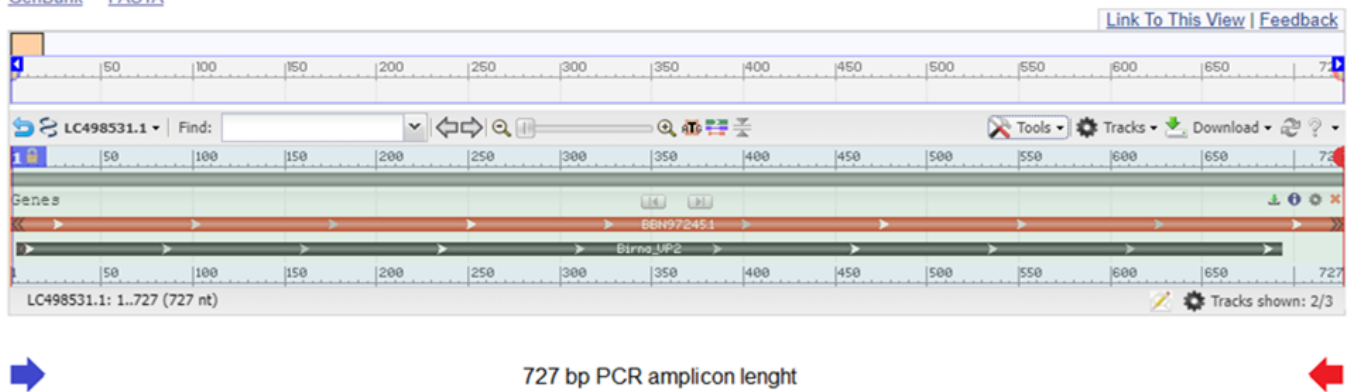


**Figure 3.** Precise locations of the VP2 locus-covering PCR amplicons within the genomic sequences of the infectious bursal disease virus in broiler chickens concerning the reference strains (GenBank accession number: LC498531.1). The red arrows point to the ends of these amplicons, while the blue arrows point to their beginnings.

**Table 1.** The length and location of the 727 bp PCR amplicons used to amplify the VP2 locus within the genomic sequences of infectious bursal disease virus in broiler chickens. The reference strains of infectious bursal disease virus (GenBank acc. no. LC498531.1)

Targeted gene	Sequences (5'-3')	Length
VP2 fragment of infectious bursal disease virus	CCAGGTGGGGGTACAATCACACTGTTCTCAGCTAATATCGATGCTATCACGAGCCTCAGCA TCGGGGGAGAACTTGTGTTTCAAACAAGCGTCCAAGGCCTTATACTGGGTGCTACCATCTA CCTTATAGGCTTTGATGGGACCGCAGTAATCACCAGAGCTGTGGCCGCAGACAATGGGCT AACGGCCGGCCTGACAACCTCATGCCATTCAATATTGTGATACCAACCAGCGAGATAAC CCAGCCAATCACATCCATCAAACCTGGAGATAGTTACCTCCAAAAGTGGTGGTCAGGCGGG GGATCAGATGTCATGGTCAGCAAGTGGGAGCTTAGCAGTGACGATTCACGGTGGCAACTA TCCAGGAGCCCTCCGTCCCCTCACACTAGTAGCCTACGAAAGAGTGGCAACAGGATCTGT CGTAACGGTCGCCGGGTGAGCAACTTCGAGCTGATTCCCAATCCTGAACTAGCAAAGAA CCTGGTCACAGAATATGGCCGATTTGACCCAGGAGCCATGAACTACACAAAATTGATACT GAGTGAGAGGGACCGTCTTGGCATCAAGACCGTATGGCCAACAAGGGAGTACACAGACTT TCGCGAGTACTTCATGGAGGTGGCCGACCTCAACTCTCCCTGAAGATTGCAGGAGCATTT GGCTTCAAAGACATAATCCGGGCCCTAAGGAGGATAGCTGTGCCGGTGGTCTCTACATTGT CCC	727 bp



**Figure 4.** DNA sequence alignment of one viral sample with its corresponding reference sequences of the PV2 locus within the infectious bursal disease virus in broiler chicken genomic sequences in comparison with reference strains of infectious bursal disease virus (GenBank acc. no. LC498531.1). The symbol “ref” refers to the NCBI reference sequences, while “S” refers to the sample code.



**Figure 5.** Amino acid residues alignment of detected variations of the VP2 protein within investigated infected broiler chickens with infectious bursal disease virus. Grey highlights refer to the amplified region of the encoded protein, blue highlights refer to the positions of silent variants detected.

**Table 2.** The details of the identified variants in the investigated sequences of the VP2 gene within infectious bursal disease virus in broiler chickens

No.	Variant	Position in PCR amplicon	position in the reference GenBank	Position in protein	Consequence/position of the variant
1.	C>T	144	144	Thr269	Silent (p.Thr269=)
2.	A>G	147	147	Ala270	Silent (p.Ala270=)
3.	C>T	204	204	Leu289	Silent (p.Leu289=)
4.	A>T	225	225	Ile296	Silent (p.Ile296=)
5.	T>G	276	276	Val313	Silent (p.Val313=)
6.	T>C	334	334	Leu333	Silent (p.Leu333=)
7.	T>C	348	348	Ile337	Silent (p.Ile337=)
8.	A>G	369	369	Gly344	Silent (p.Gly344=)
9.	A>T	426	426	Val363	Silent (p.Val363=)
10.	T>C	459	459	Ile374	Silent (p.Ile374=)
11.	C>A	462	462	Pro375	Silent (p.Pro375=)
12.	T>C	498	498	Tyr387	Silent (p.Tyr387=)
13.	A>T	597	597	Thr420	Silent (p.Thr420=)

The letter “S #” refers to the VIRAL sample code. Identified variants were named according to the international nomenclature system. P: Protein

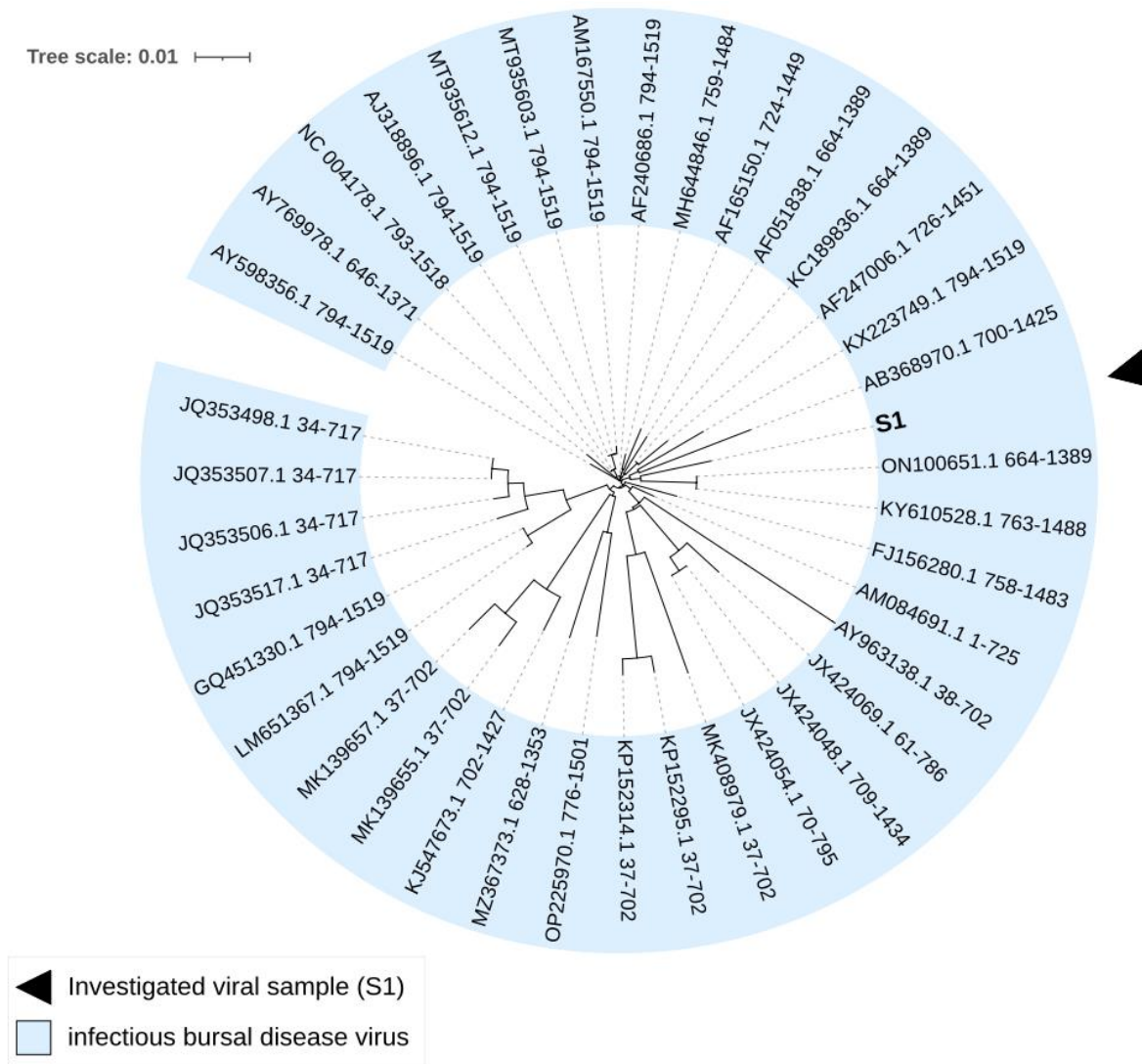


**Figure 6.** The entire circular phylogenetic tree indicated that genetic variations of the PV2 locus in a single infectious bursal disease virus isolate in broiler chickens. The left-hand portion of the tree's scale represents the degree of phylogenetic positions among the viral organisms classified in the tree. The code of the examined samples was indicated by the letter "S".

### Histopathological results

#### Bursa of Fabricius

The histopathological lesions were observed in the bursa of Fabricius. These pathological changes indicated an obvious degeneration of the bursal epithelium associated with hemorrhage, and cystic cavities were observed, particularly in the follicular and epithelium of the bursa of Fabricius (Figure 7). The epithelial bursa showed thickening, and the cell hyperplasia encompassed some cystic structures. Follicles contained an abundance of inflammatory cells, mainly heterophils that were observed within follicles, along with macrophages in the inter-follicular spaces (Figure 8). Clear coagulative necrosis was detected in the interior follicular bursa, developing in areas occupied by eosinophilic materials. It

also appeared that the cortical follicular regions contained a low density of heterophilic cells, compared to many cells located in the medullary follicular regions associated with macrophages and eosinophilic homogenous substances (Figure 8).

#### Lungs

The pathological lesions in the lung tissues displayed moderate to severe inflammation, combined with significant congestion and edema. Additionally, there was substantial fluid accumulation. In parenchymal cells of the lung tissues, both multifocal necrosis and mononuclear inflammatory cellular infiltration were seen (Figure 8). Several of the air capillaries exhibited thicker walls and/or parenchymal degeneration, both of which were associated with pronounced edema and congestion.



**Kidney**

Infected chickens with IBD had clear histological changes in their kidneys, such as bleeding and severe congestion in the subcapsular region, as well as edema caused by the breakdown of the epithelial cells that line tubules and ducts in some places (Figure 9). The epithelium tissue of lining tubules and ducts of the kidney also contained this protein. There was also apparent hyperplasia in some of the renal epithelium and localized mononuclear infiltration of cells. The proximal and distal convoluted tubules and ducts indicated eosinophilic casts. Cortical kidney tissue demonstrated signs of nephritis and glomeruli degeneration (Figure 9).

**Liver**

In the liver, the pathological changes indicated massive degeneration and severe inflammation, along with infiltration with mononuclear inflammatory cells as can be seen in Figure 10. There were many cystic cavities observed in the liver parenchyma. These cavities were detected diffusely in superficial and deep parenchymal tissues associated with severe congestion and hemorrhage (Figure 10). There were also clear periportal aggregations of heterophils, commonly perivascular.

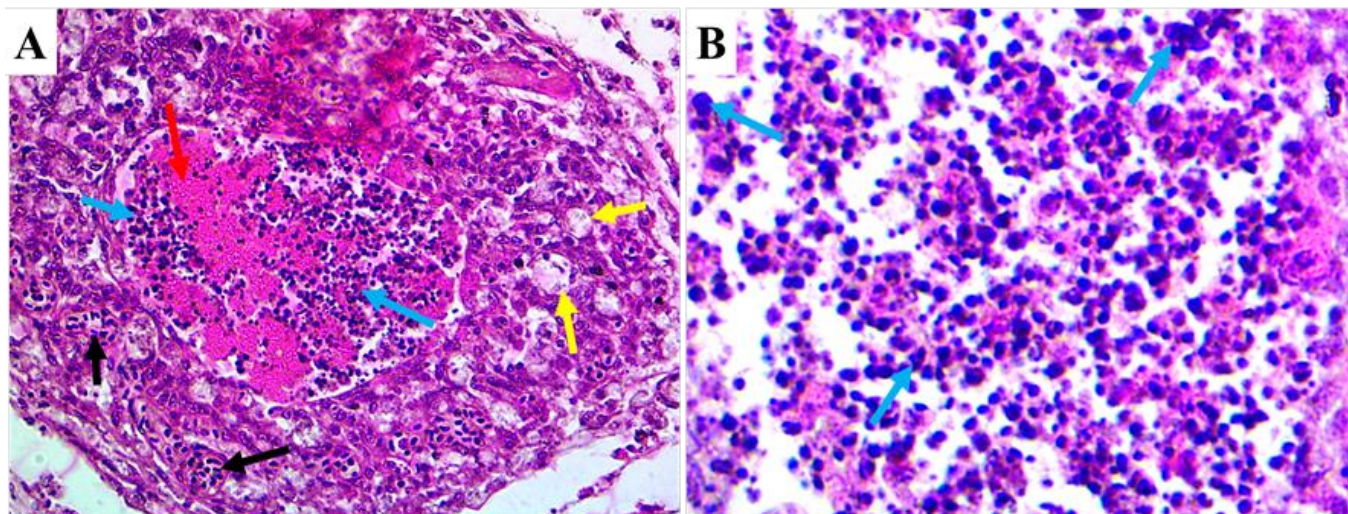


**Figure 7.** Histological changes of the bursa of Fabricius in chickens infected with infectious bursal disease virus. **A** and **B** indicate a clear degeneration and necrosis in the follicular bursa. Black arrows indicated severe congestion, red arrow showed eosinophilic homogenous material in the medullary region, yellow arrows indicated cystic cavities, whereas traquaze arrows present mononuclear inflammatory cells mainly heterophils and macrophage (**A** at 40X magnification, **B** at 60X magnification).

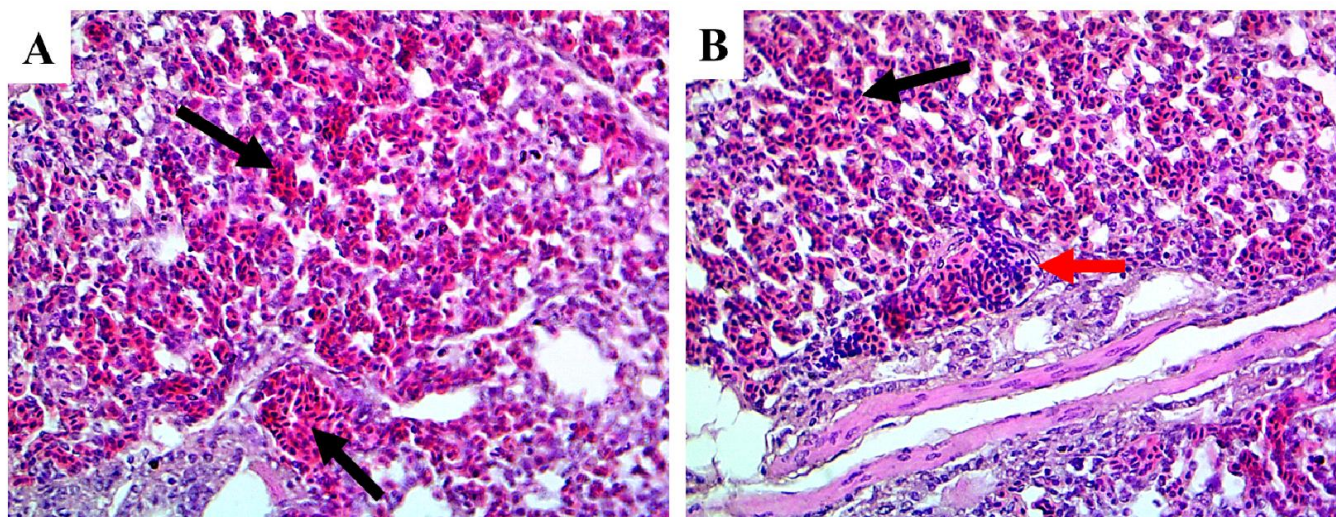


**Figure 8.** Pathological changes in infected broiler chickens with infectious bursal disease virus. **A** and **B** indicate severe inflammation of the lung parenchyma associated with severe congestion (black arrows) and infiltration with inflammatory cells represented by a red arrow (40x magnification).

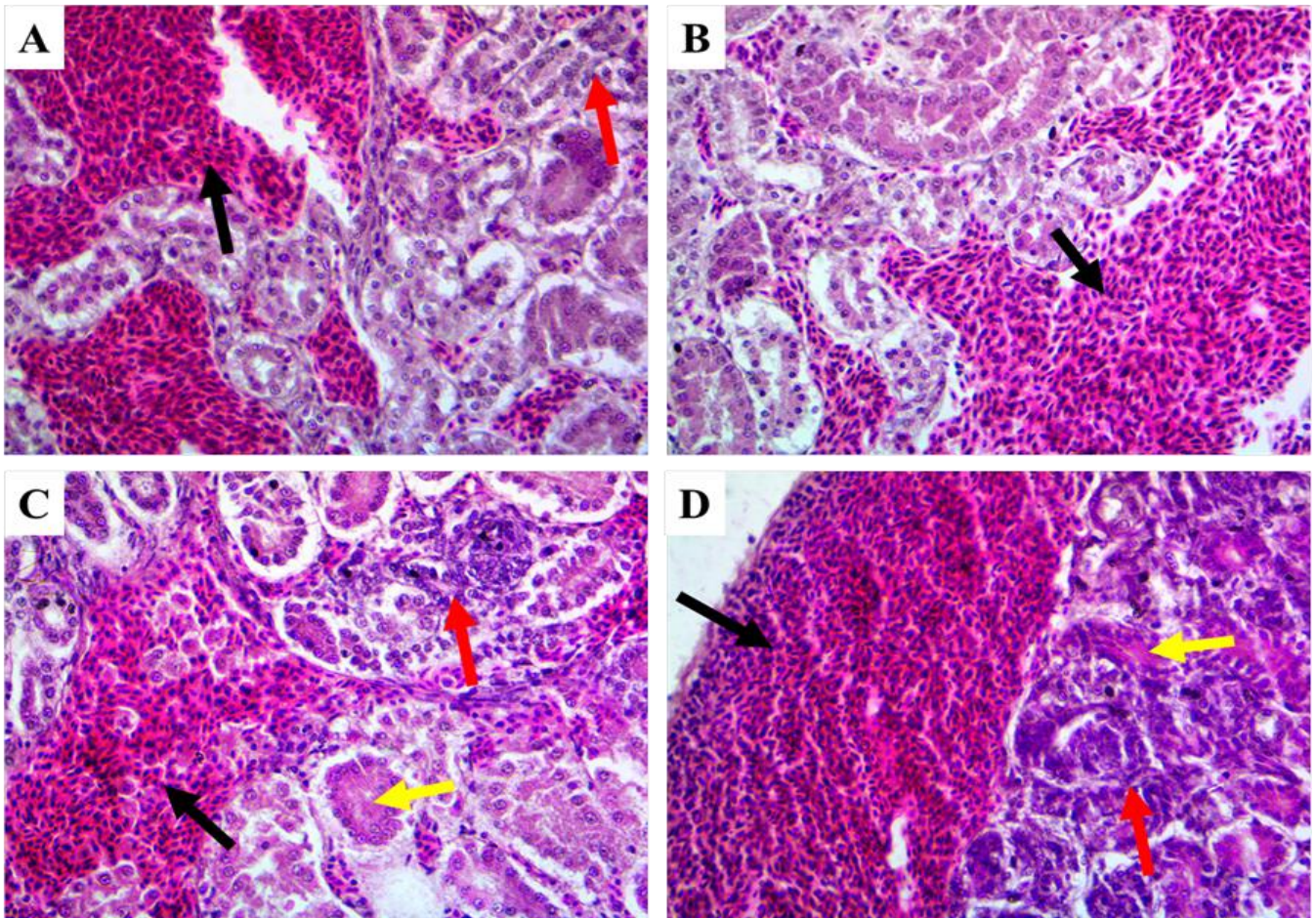


**Figure 9.** Histological changes in the kidney of broiler chickens infected with infectious bursal disease virus. **A**, **B**, and **C** show the pathological changes presented in the medullary region accompanied by severe hemorrhage (black arrows), eosinophilic casts (yellow arrows), and severe congestion was observed in the subcapsular area appeared clearly (**D**), red arrows indicated multifocal necrosis and severe degeneration and necrosis in the renal epithelium (40x magnification).

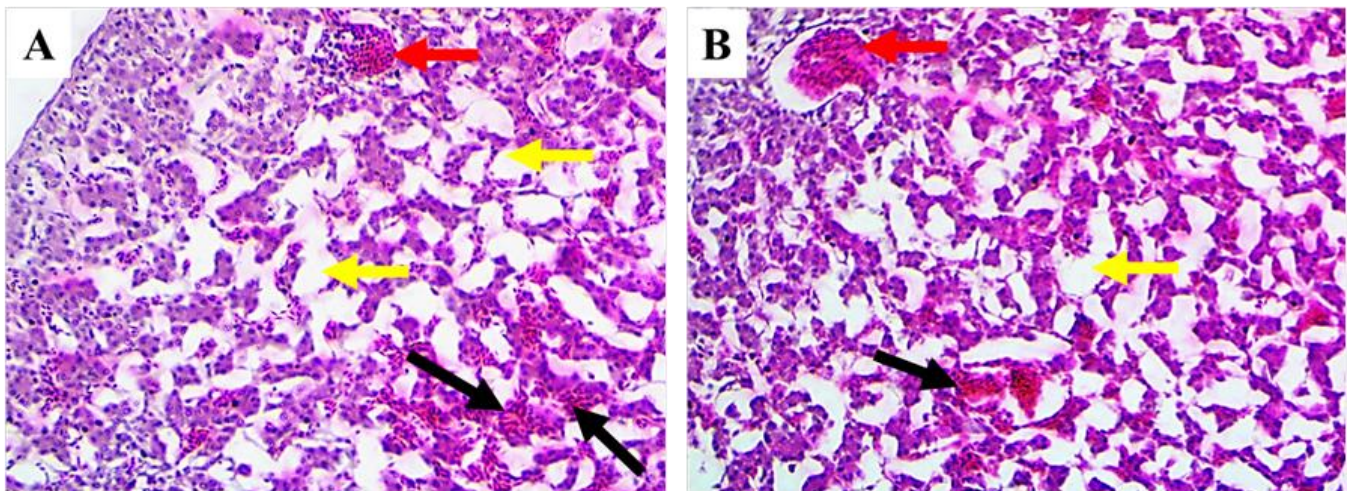


**Figure 10.** Histopathological lesions in the liver of broiler chickens infected with infectious bursal disease virus. **A** and **B**: Pathological changed appeared as a massive degeneration and necrosis in hepatocytes accompanied by severe infiltration and congestion (black arrows), and many mononuclear inflammatory cells (red arrows), whereas yellow arrows represented the development of many cystic cavities observed diffused in the superficial and deep parenchymal tissues (40x magnification).

## DISCUSSION

Due to improper vaccination administration and insufficient vaccine evaluation, the IBDV remains a significant threat to the global chicken industry. Despite the possibility of infection in guinea pigs, ostriches, turkeys, ducks, and ducklings, the clinical condition only affects chickens (Müller et al., 2012; Al-Zuhariy et al., 2016). In chickens younger than 3 weeks of age, the disease typically presents as less severe or subclinical, whereas birds between 3 and 6 weeks of age often experience severe acute disease with significant mortality rates (Müller et al., 2012). The present study demonstrated that vvIBDV remains a substantial financial threat to the poultry sector across various regions within the Diyala Governorate, in addition to the other areas not specifically addressed in this research. High mortality rates were observed in all broiler flocks despite the widespread use of vaccines against the disease.

Using oligonucleotide primers selected from the highly conserved region PCR was widely used to successfully amplify the IBDV VP2 gene region, followed by sequence analysis and phylogenetic tree comparisons (Mawgod et al., 2014; Techera et al., 2019).

It has been essential to use the molecular characterization of the very virulent IBDV to examine global trends in the prevalence, evolution, and field status of the virus to effectively control IBD in broilers (Cheggag et al., 2020). The IBDV high genetic and antigenic diversity, the VP2 protein is widely used for phylogenetic genotyping and grouping of IBDV strains, either by using its entire nucleotide sequence or the sequence of its hypervariable region (VP2-HRV; Jackwood et al., 2018). This offered a helpful molecular replacement for dividing apart IBDV strains (Van den Berg, 2000). Using the method outlined by Meir et al. (2001), amplification of this gene was reduced. The VP2 gene was amplified using primers (IBDf and IBDr), which produced the anticipated DNA product of 727 bp in length. These findings were in line with those made public by other researchers (Moody et al., 2000; Zierenberg et al., 2001; Mawgod et al., 2014). These studies suggested that the major capsid protein of IBDV, VP2, harbors crucial immunodominant epitopes necessary for eliciting neutralizing antibodies against the virus. The IBDV isolates were classified into various antigenic subtypes and genotypes with the aid of antigenic and molecular analysis of this portion of the protein. The IBDV consists of two segments (A and B) according to Li et al. (2015) and Cheggag et al. (2020). In nature, viruses with fragmented genomes often exchange genetic material when they infect the same cell concurrently. Contrasting

the local sample (GenBank acc. No. LC498531.1) with reference sequences of the IBDV revealed the presence of 13 nucleic acid variants.

The VP2 coat protein of the IBDV was translated to contain the sequences of the investigated nucleic acids at the appropriate places. Amino acid alignment of these amino acid sequences with its reference sequences indicated that the investigated 727 bp amplicons consisted of 242 amino acid sequences in the entire amino acid sequences in the VP2 in IBDV. It was found that all the detected variants had caused a silent effect in the VP2 protein. The majority of naturally occurring IBDV strains exhibit intermediate virulence levels, falling between strains of the classic pathotype and extremely virulent variants.

Due to the rapid mutation rate of RNA viruses and the significant selection pressure induced by widespread bird immunization, viruses may acquire distinct characteristics enabling them to thrive within immune populations (Dennehy, 2017). Changes in the virulence of circulating IBDV strains were caused by these mutations, which also caused antigenic variation. Consequently, it was imperative to promptly detect and describe newly discovered IBDV isolates, comparing them to previously documented viruses (van den Berg, 2000). Due to the IBDV's multiple clades being present in this study, a direct comparison between the local sample and the previously established reference genotypes was made to ascertain the precise positioning of the sample within the major clades of these viral particles. A thorough phylogenetic tree was constructed using the observed nucleic acid sequences present in the examined sample. Incredibly helpful genetic distances between all samples being studied were displayed on the neighbor-joining comprehensive tree that was being built. Most notably, the presence of a specific phylogenetic positioning in the locally examined sample may suggest that the VP2 fragment had a specific function in the evolution of IBDV sequences to attack broiler chickens (Zhang et al., 2000).

The current study revealed that the local IBDV sample under investigation, which was identified as S1, was incorporated within a specific position of the constructed tree within a clade formed of five samples of a group of very virulent IBDV strains. Within this clade, it deserved to be noted that all these five samples were suited in the vicinity of variable reference sequences deposited from variable IBDV strains of India (GenBank KX223749.1), Tanzania (GenBank AB368970.1), Hungary (GenBank ON100651.1), and Egypt (GenBank KY610528.1) origins within this clade. However, no close

phylogenetic positioning of the present sample toward these isolates was found. A different investigation found that the local isolate Diyala/VP2/MW883071 from the same region of the current study and the reference isolate (MF142560.1) were the most comparable to each other (Al-Azzawi et al., 2021). This local isolate, Diyala/VP2/MW883071, had a sequence alignment with their corresponding partial VP2 strains from NCBI 710-Jordan (MF142560.1), incorporated within a specific position in one cluster with the group of very virulent IBDV strains from the USA, primarily vvIBDV pathotype or vvIBDV reassortment strains, with an estimated 99.2% similarity between them (Al-Azzawi et al., 2021). The findings of Samy et al. (2020), who discovered that IBDV was present in nine out of ten samples collected during an IBD outbreak in the summer of 2015, were supported by these findings. The bulk of the Egyptian isolates belonged to the vvIBDV-related clade and were grouped with the antigenically changed vvIBDV strains, per phylogenetic analysis based on incomplete VP2 sequences. Additionally, based on the nucleotide sequences of HVR VP2, the current results were in agreement with those of Zierenberg et al. (2001). This region of the protein was subjected to antigenic and molecular investigation, which assisted in grouping the IBDV isolates into various antigenic subtypes.

Histopathological analysis of lymphoid tissue from infected chickens with IBD revealed that acute necrosis in the follicular bursa was linked to a decrease in lymphoid cells as well as severe interfollicular congestion and hemorrhage. Aliyu et al. (2022) demonstrated similar alterations in highly pathogenic IBDVs in chickens. Certain viral receptors on B cells, which were mostly present in the lymphoid follicles, may be responsible for the extensive damage seen in the bursa lymphoid follicles (Li et al., 2023). The findings of this study supported the argument posited by other researchers (Withers et al., 2005; Hasan and Ali, 2015) that B cells serve as the main target of IBD infection. Although similar pathological abnormalities in the bursal follicles have been observed before with Withers et al. (2005), the severity of these changes was greater. Additionally, bursal atrophy was primarily characterized by the degeneration of follicles of lymphoid tissue and the subsequent disintegration and deterioration of B cells (Li et al., 2023). The induction of alterations in the bursa's cytokine concentrations by the IBDV has been observed, suggesting that this phenomenon leads to the promotion of inflammatory response and disruption inside the tissue microenvironment (Huang et al., 2021). These changes

serve as a strategic mechanism employed by the virus to diminish the activity of B lymphocytes, therefore evading or suppressing the immunological responses mounted by the host (Huang et al., 2021; Li et al., 2023). Non-lymphoid tissues (liver, lungs, and kidneys) indicated the same severe inflammation and multifocal necrosis as well as mononuclear inflammatory cells in the present histological results. Some studies have shown that the ability of IBD to induce such histological damage in non-lymphoid tissues could be interpreted as a potential property of hyper-virulent IBD which was consistent with the current published results (Silva et al., 2015; Damairia et al., 2023). However, the generalized pyknosis and tubular necrosis of the epithelial cells, along with severe necrosis and hemorrhage in the liver observed in the present study, appear to be more pathogenic than already demonstrated for the non-lymphoid organs in IBD infection (Al-Zuhariy et al., 2016; Yasmin et al., 2016). Hence, these extensive lesions in non-lymphoid organs could directly contribute to the elevated mortality rates observed during gross inspections, potentially leading to a widespread outbreak within the flock.

## CONCLUSION

In this study, IBDV was identified and characterized in broiler chickens across multiple farms in the Diyala Governorate of Iraq. Employing molecular techniques such as RT-PCR targeting the VP2 gene, IBDV was detected in 10 out of 15 samples, with one strain assigned an accession number in the NCBI database. Phylogenetic analysis unveiled three distinct groups, with regional samples (S1) forming a closely related cluster of five samples, indicative of the local circulation of IBDV strains in the study area. Histopathological examination of the bursa of Fabricius, lungs, liver, and kidneys revealed significant pathological changes, including degeneration, necrosis, and infiltration of inflammatory cells, particularly heterophils. These findings offer compelling evidence of the disease and correlate with the observed clinical symptoms in affected chickens, which include depression, bleeding, and bursa enlargement.

## DECLARATIONS

### Acknowledgments

Appreciation is expressed to the dedicated workers in all college laboratories and the experimental animal room for their invaluable assistance throughout this study. Moreover, thanks are extended to all members of the

Department of Microbiology, College of Veterinary Medicine, University of Diyala, for their respected logistical support, which contributed to the successful completion of this research.

### Funding

The research was funded by the College of Veterinary Medicine, Diyala University, Iraq, as well as by the private resources of the research participants.

### Availability of data and materials

For access to the data and materials used in this study, interested individuals can reach out to the corresponding author directly. Instead, the data may also be available through a designated data source.

### Ethical considerations

Ethical considerations, such as plagiarism, consent for publication, misconduct, data fabrication and/or forgery, double publication and/or submission, and replication, were thoroughly addressed by all authors.

### Authors' contributions

The research team for this study comprised Ammar T. Nasser, Amer Al-Azzawi, and Karim Al-Ajeeli, who contributed to the molecular biology aspects of the investigation. Ramzi Al-Agele provided expertise in histology and histopathology. The manuscript was collaboratively written by Ammar T. Nasser, Amer Al-Azzawi, and Ramzi Al-Agele, consolidating their collective insights from the molecular and histological analyses. All authors checked the last edition of the article before publication.

### Competing interests

The authors declare that they have no conflict of interest.

## REFERENCES

- Al-Azzawi AK, Nasser AT, and Al-Ajeeli KS (2021). Molecular detection of infectious bursal disease virus in broiler chickens of Diyala Province, Iraq. *Journal of World's Poultry Research*, 11(4): 439-445. DOI: <https://www.doi.org/10.36380/jwpr.2021.52>
- Aliyu HB, Hamisu TM, Hair Bejo M, Omar AR, and Ideris A (2022). Comparative pathogenicity of Malaysian variant and very virulent infectious bursal disease viruses in chickens. *Avian Pathology*, 51(1): 76-86. DOI: <https://www.doi.org/10.1080/03079457.2021.2006604>
- Allan WH, Faragher JT, and Cullen GA (1972). Immunosuppression by infectious bursal agent in chickens immunized against Newcastle disease. *Veterinary Record*, 90(18): 511-512. DOI: <https://www.doi.org/10.1136/vr.90.18.511>
- Al-Sheikhly F, Mutalib AA, and Rasheed DK (1978). Infectious bursal disease in chickens. 4 annual conference of Iraq Veterinary Medicine Association, Baghdad, pp: 13.
- Al-Zuhariy MTB, Abdulmaged SH, Rabee RHS, and Al-Baldawi AAA (2016). Molecular genotyping of infectious bursal disease virus (IBDV) isolated from layer flocks in Iraq. *Al-Anbar Journal of Veterinary Sciences*, 9(2): 100-109. Available at: <https://www.iasj.net/iasj/download/2efb0ee0f4decb8f>
- Cao YC, Yeung WS, Law M, Bi YZ, Leung FC, and Lim BL (1998). Molecular characterization of seven Chinese isolates of infectious bursal disease virus: classical, very virulent, and variant strains. *Avian Diseases*, 42(2): 340-351. DOI: <https://www.doi.org/10.2307/1592484>
- Cheggag M, Zro K, Terta M, Fellahi S, Mouahid M, El Houadfi M, Sebbar G, and Kichou F (2020). Isolation, molecular and pathological characterization of infectious bursal disease virus among broiler chickens in Morocco. *Journal of World's Poultry Research*, 10(3): 493-506. DOI: <https://www.doi.org/10.36380/jwpr.2020.57>
- Coulibaly F, Chevalier C, Gutsche I, Pous J, Navaza J, Bressanelli S, Delmas B, and Rey FA (2005). The birnavirus crystal structure reveals structural relationships among icosahedral viruses. *Cell*, 120(6): 761-772. DOI: <https://www.doi.org/10.1016/j.cell.2005.01.009>
- Damairia BA, Putri K, and Wibowo MH (2023). Examination of macroscopic and microscopic lesions in IBDV-infected organs and molecular characterization of IBDV VP1 gene fragments obtained from commercial broiler farms in Indonesia. *Veterinary World*, 16(5): 1061-1070. DOI: <https://www.doi.org/10.14202/vetworld.2023.1061-1070>
- Dennehy JJ (2017). Evolutionary ecology of virus emergence. *Annals of the New York Academy of Sciences*, 1389(1): 124-146. DOI: <https://www.doi.org/10.1111/nyas.13304>
- Deorao CV, Rajasekhar R, Ravishankar C, Nandhakumar D, Sumod K, Palekkodan H, John K, and Chaithra G (2021). Genetic variability in VP1 gene of infectious bursal disease virus from the field outbreaks of Kerala, India. *Tropical Animal Health and Production*, 53(3): 407. DOI: <https://www.doi.org/10.1007/s11250-021-02852-7>
- Dey S, Pathak DC, Ramamurthy N, Maity HK, and Chellappa MM (2019). Infectious bursal disease virus in chickens: Prevalence, impact, and management strategies. *Veterinary Medicine: Research and Reports*, 2019(10): 85-97. DOI: <https://www.doi.org/10.2147/vmr.s185159>
- Fauquet CM and Mayo MA (2001). The 7th ICTV Report. *Archives of Virology*, 146(1): 189-194. DOI: <https://www.doi.org/10.1007/s007050170203>
- Ferrero D, Garriga D, Navarro A, Rodríguez JF, and Verdaguer N (2015). Infectious bursal disease virus VP3 upregulates VP1-mediated RNA-dependent RNA replication. *Journal of Virology*, 89(21): 11165-11168. DOI: <https://www.doi.org/10.1128/jvi.00218-15>
- Hasan II and Ali BH (2015). Histological effect of infectious bursal disease virus on bursa of fabricia, Thymus gland and bone marrow tissues with monitoring of virus antibodies

- level during experimental infection on broiler chicken. *Tikrit Journal of Pure Science*, 20(2): 44-48. DOI: <https://www.doi.org/10.25130/tjps.v20i2.1157>
- Huang X, Liu W, Zhang J, Liu Z, Wang M, Wang L, Zhou H, Jiang Y, Cui W, Qiao X et al. (2021). Very virulent infectious bursal disease virus-induced immune injury is involved in inflammation, apoptosis, and inflammatory cytokines imbalance in the bursa of fabricius. *Developmental & Comparative Immunology*, 114: 103839. DOI: <https://www.doi.org/10.1016/j.dci.2020.103839>
- Ingrao F, Rauw F, Lambrecht B, and van den Berg T (2013). Infectious bursal disease: A complex host-pathogen interaction. *Developmental & Comparative Immunology*, 41(3): 429-438. DOI: <https://www.doi.org/10.1016/j.dci.2013.03.017>
- Jackwood DJ and Sommer-Wagner S (2007). Genetic characteristics of infectious bursal disease viruses from four continents. *Virology*, 365(2): 369-375. DOI: <https://www.doi.org/10.1016/j.virol.2007.03.046>
- Jackwood DJ, Schat KA, Michel LO, and de Wit S (2018). A proposed nomenclature for infectious bursal disease virus isolates. *Avian Pathology*. 47(6): 576-584. DOI: <https://www.doi.org/10.1080/03079457.2018.1506092>
- Jasim KA, Al-Azzawi AK, Kadhim TJ, and AL-Ajeeli KS (2022). Phylogenetic analysis of RT-PCR detected infectious bronchitis virus locally infected broiler farms in Diyala Governorate-IRAQ. *International Journal of Health Sciences*, 6(S1): 9747-9762. DOI: <https://www.doi.org/10.53730/ijhs.v6nS1.7279>
- Kadhim TJ, Al-Agele RAA, and Ibrahim RS (2023). Histopathological study of the cecal tonsils post newcastle vaccine in broiler chickens. *AIP Conference Proceedings*, 2475(1): 100008. DOI: <https://www.doi.org/10.1063/5.0103023>
- Lasher HN and Shane SM (1994). Infectious bursal disease. *World's Poultry Science Journal*, 50(2): 133-166. DOI: <https://www.doi.org/10.1079/wps19940013>
- Letunic I and Bork P (2019). Interactive tree of life (iTOL) v4: Recent updates and new developments. *Nucleic Acids Research*, 47(W1): W256-W259. DOI: <https://www.doi.org/10.1093/nar/gkz239>
- Li Y, He L, Cheng X, Li J, Jia Y, and Yang D (2015). Histamine levels in embryonic chicken livers infected with very virulent infectious bursal disease virus. *Veterinary Immunology and Immunopathology*, 168(1-2): 91-96. DOI: <https://www.doi.org/10.1016/j.vetimm.2015.08.012>
- Li K, Niu X, Jiang N, Zhang W, Wang G, Li K, and Wang X (2023). Comparative pathogenicity of three strains of infectious bursal disease virus closely related to poultry industry. *Viruses*, 15(6): 1257. DOI: <https://www.doi.org/10.3390/v15061257>
- Lukert PD and Saif YM (2003). Infectious bursal disease. In: Y. M. Saif (Editor), *Disease of poultry*, 11th Edition. Iowa State University Press., Ames, IA, USA, pp. 161-180.
- Mawgod SA, Arafa AS, and Hussein HA (2014). Molecular genotyping of the infectious bursal disease virus (IBDV) isolated from broiler flocks in Egypt. *International Journal of Veterinary Science and Medicine*, 2(1): 46-52. DOI: <https://www.doi.org/10.1016/j.ijvsm.2014.02.004>
- Meir R, Jackwood DJ, and Weisman Y (2001). Molecular typing of infectious bursal disease virus of Israeli field and vaccine strains by the reverse transcription/polymerase chain reaction/restriction fragment length polymorphism assay. *Avian Diseases*, 45(1): 223-228. DOI: <https://www.doi.org/10.2307/1593032>
- Moody A, Sellers S, and Bumstead N (2000). Measuring infectious bursal disease virus RNA in blood by multiplex real-time quantitative RT-PCR. *Journal of Virological Methods*, 85(1-2): 55-64. DOI: [https://www.doi.org/10.1016/s0166-0934\(99\)00156-1](https://www.doi.org/10.1016/s0166-0934(99)00156-1)
- Müller H, Mundt E, Eterradosi N, and Islam MR (2012). Current status of vaccines against infectious bursal disease. *Avian Pathology*, 41(2): 133-139. DOI: <https://www.doi.org/10.1080/03079457.2012.661403>
- Raja P, Senthilkumar TMA, Parthiban M, Thangavelu A, Gowri AM, Palanisammi A, and Kumanan K (2016). Complete genome sequence analysis of a naturally reassorted infectious bursal disease virus from India. *Genome Announcements*, 4(4): e00709-16. DOI: <https://www.doi.org/10.1128/genomea.00709-16>
- Rauf A, Khatri M, Murgia MV, and Saif YM (2011). Expression of perforin-granzyme pathway genes in the bursa of infectious bursal disease virus-infected chickens. *Developmental & Comparative Immunology*, 35(5): 620-627. DOI: <https://www.doi.org/10.1016/j.dci.2011.01.007>
- Samy A, Courtilon C, Briand FX, Khalifa M, Selim A, Arafa AES, Hegazy A, Eterradosi N, and Soubies SM (2020). Continuous circulation of an antigenically modified very virulent infectious bursal disease virus for fifteen years in Egypt. *Infection, Genetics and Evolution*, 78: 104099. DOI: <https://www.doi.org/10.1016/j.meegid.2019.104099>
- Techera C, Tomás G, Panzera Y, Banda A, Perbolianachis P, Pérez R, and Marandino A (2019). Development of real-time PCR assays for single and simultaneous detection of infectious bursal disease virus and chicken anemia virus. *Molecular and Cellular Probes*, 43: 58-63. DOI: <https://www.doi.org/10.1016/j.mcp.2018.11.004>
- van den Berg TP (2000). Acute infectious bursal disease of chicken. *Areview. Avian Pathology*, 29(3): 175-194. DOI: <https://www.doi.org/10.1080/03079450050045431>
- Wang Y, Wu X, Li H, Wu Y, Shi L, Zheng X, Luo M, Yan Y, and Zhou J (2009). Antibody to VP4 protein is an indicator discriminating pathogenic and nonpathogenic IBDV infection. *Molecular Immunology*, 46(10): 1964-1969. DOI: <https://www.doi.org/10.1016/j.molimm.2009.03.011>
- Withers DR, Young JR, and Davison TF (2005). Infectious bursal disease virus-induced immunosuppression in the chick is associated with the presence of undifferentiated follicles in the recovering bursa. *Viral Immunology*, 18(1): 127-137. DOI: <https://www.doi.org/10.1089/vim.2005.18.127>
- Yasmin A, Yeap S Hair-Bejo M, and Omar A (2016). Characterization of chicken splenic-derived dendritic cells following vaccine and very virulent strains of infectious bursal disease virus infection. *Avian Diseases*, 60(4): 739-751. <https://www.doi.org/10.1637/11275-091315-reg.1>
- Zhang Z, Schwartz S, Wagner L, and Miller W (2000). A greedy algorithm for aligning DNA sequences. *Journal of*

Computational Biology, 7(1-2): 203-214. DOI:  
<https://www.doi.org/10.1089/10665270050081478>

Zhang W, Wang X, Gao Y, and Qi X (2022). The over-40-years-epidemic of infectious bursal disease virus in China. Viruses, 14(10): 2253. DOI:  
<https://www.doi.org/10.3390/v14102253>

Zierenberg K, Raue R, and Muller H (2001). Rapid identification of very virulent strains of infectious bursal disease virus by reverse transcription-polymerase chain reaction combined with restriction enzyme analysis. Avian Pathology, 30(1): 55-62. DOI:  
<https://www.doi.org/10.1080/03079450020023203>

**Publisher's note:** [Scieline Publication](#) Ltd. remains neutral with regard to jurisdictional claims in published maps and institutional affiliations.



**Open Access:** This article is licensed under a Creative Commons Attribution 4.0 International License, which permits use, sharing, adaptation, distribution and reproduction in any medium or format, as long as you give appropriate credit to the original author(s) and the source, provide a link to the Creative Commons licence, and indicate if changes were made. The images or other third party material in this article are included in the article's Creative Commons licence, unless indicated otherwise in a credit line to the material. If material is not included in the article's Creative Commons licence and your intended use is not permitted by statutory regulation or exceeds the permitted use, you will need to obtain permission directly from the copyright holder. To view a copy of this licence, visit <https://creativecommons.org/licenses/by/4.0/>.

© The Author(s) 2023